Maize Stem Tissues: Cell Wall Concentration and Composition during Development

H. G. Jung* and M. D. Casler

ABSTRACT

Grass maturation results in reduced cell wall degradability by ruminant livestock. Using a specific internode of maize (*Zea mays* L.) stems as a model, the pattern of grass stem tissue and cell wall development was characterized. The fourth elongated internode above ground level from three maize hybrids was sampled at 10 stages of development beginning when the internode was about 10 mm in length through physiological maturity from a 2-yr, replicated field trial at St. Paul, MN. Tissue development was characterized by light microscopy. Cell wall concentration and composition (polysaccharide sugar residues, lignin, ferulates, and *p*-coumarates) were determined. Internode length and cross-sectional area increased from Sampling Date 1 until the interval between Sampling Dates 5 and 6. During elongation only protoxylem vessels stained positive for lignin. After elongation, parenchyma, sclerenchyma, and metaxylem tissues lignified, but phloem did not. Cell wall concentration increased until shortly after elongation ended. Cell wall lignin concentration declined over the first four samples, with an increase in glucose and xylose polysaccharide residues, before rising sharply until after elongation was complete. Ferulate cross-links of lignin to arabinoxylan increased 12-fold during elongation. Our results indicated that post-elongation development of sclerenchyma and rind-region parenchyma accounted for the majority of cell wall accumulation and lignification in maize stems.

A S FORAGE crops mature the concentration of cell wall material in the herbage increases and cell wall composition changes (Aman and Lindgren, 1983). Degradability of forage cell walls by rumen microorganisms declines with maturity. Deposition of lignin in cell walls is generally regarded as the primary cause of this reduction in potential ruminal degradation, although other changes in cell wall structure such as ferulate cross-linkages in grasses and lignin composition, have been suggested to play a role (Jung and Deetz, 1993). While the negative correlation of lignin concentration and cell wall degradability is commonly observed across maturity stages, this relationship is not reliably seen with forages of similar maturity (Jung and Buxton, 1994; Jung et al., 1994). Although it is clear that the presence of lignin in cell walls negatively impacts forage degradability, questions remain as to the exact causes of this effect.

Leaves and stems of forages are composed of a variety of tissues and the degradability of these tissues dif-
fers (Akin, 1989). Presence of lignin in plant tissues is generally assessed using histological stains such as acid phloroglucinol (Jensen, 1962). In mature grass stems, discrete vascular bundles contain lignified proto- and metaxylem tissues and nonlignified phloem tissue (Wilson, 1993). Lignified sclerenchyma fibers surround the vascular bundles. The vascular tissue of legume stems consists of a continuous xylem tissue ring with vessel and fiber cells, and phloem tissue consists of cell bundles on the opposite side of the cambial layer from the xylem. Xylem vessels and fibers are lignified in legumes; however, phloem fiber cells are only partially lignified and secondary phloem is not lignified (Wilson, 1993).

Jung and Engels (2002) demonstrated that deposition of lignified xylem tissue in alfalfa (*Medicago sativa* L.) stems caused by cambial activity after internode elongation was complete, accounted for almost all the reduction in cell wall degradability observed during development of this forage. The nonlignified tissues in alfalfa were shown to remain completely and rapidly degradable throughout stem development, and these tissues were rich in pectin (Engels and Jung, 1998; Jung and Engels, 2001, 2002). These data explain why legumes such as alfalfa have rapid rates of cell wall degradation, but the cell walls are of limited potential extent of degradability (Buxton, 1989).

While there are extensive data in the literature on chemical composition of cell walls and the differences in degradability of various tissues for grass forages, this information has not yet led to an understanding of how cell wall development of grass tissues results in the observed patterns of reduced ruminal degradability. As genetic improvement of forage quality moves toward a more molecular approach, such detailed knowledge of the interactions between tissue and cell wall development, and their impacts on degradability will be needed for accurate targeting of gene manipulation. A study was conducted to describe the patterns of grass stem tissue and cell wall development using a specific maize internode, and relate these developmental patterns to degradation of the tissues and cell walls by rumen microorganisms. The objective was to identify key internode tissues and stages of development that determine stem cell wall degradability. Rates of deposition for the individual cell wall components during development of whole maize internodes were reported earlier (Jung, 2003). Developmental patterns for individual tissues and internode cell wall composition are reported here, with an emphasis on the pattern of lignification. Data on degradability of maize internode tissues and cell walls are described in a companion paper (Jung and Casler, 2006).

H.G. Jung, USDA-ARS Plant Science Res. Unit and U.S. Dairy Forage Res. Center Cluster, Univ. of Minnesota, Dep. of Agronomy and Plant Genetics, 411 Borlaug Hall, 1991 Upper Buford Circle, St. Paul, MN 55108; M.D. Casler, USDA-ARS U.S. Dairy Forage Res., 1925 Linden Drive West, Madison, WI 53706. Mention of a proprietary product does not constitute a recommendation or warranty of the product by the USDA or the University of Minnesota, and does not imply approval to the exclusion of other suitable products. Received 8 Feb. 2006. *Corresponding author (jungx002@umn.edu).

Abbreviations: OM, organic matter; LSD, least significant difference.

MATERIALS AND METHODS

Plant Material

Three non-related maize hybrids (A632 × A619, A679 × FR481, and Mycogen 2677; referred to as hybrids 632, 679, and 2677, respectively) of similar relative maturity were planted on the University of Minnesota St. Paul campus 14 May 1998 and 19 May 1999. In both years the field plot design was a randomized complete block with two replications for each maize hybrid. Plots consisted of eight rows with 44 seeds per row at a spacing of 23 cm within rows and 76 cm between rows. The soil was a Waukegan silt loam (fine-silty over sandy or sandy-skeletal, mixed, superactive, mesic Typic Hapludoll). Plots were fertilized before planting according to soil test results and University of Minnesota recommendations for maize production. A pre-emergence herbicide was applied to the plots before planting and mechanical weed control was done during the growing season.

Beginning in mid-June of both years, randomly chosen maize plants were examined for stage of development of the fourth elongated internode above the soil surface. Sampling was initiated when this internode was 10 to 15 mm in length and plants had reached the V8 (eight expanded leaves) stage of development (Ritchie et al., 1989). Ten samples of the fourth elongated internode above ground level were taken over the course of the growing season (Table 1). Number of internodes collected was greater at earlier stages of development to ensure sufficient sample material for subsequent analyses.

Maize plants were cut at ground level and the position of the fourth elongated internode above ground level was determined by visual inspection of the basal stem internodes. The internode was excised from the stem by cutting through the nodes. The length of four randomly chosen internodes was measured with a ruler. Diameter of these four internodes was measured with calipers in the middle of the internode, across both the long and short axes. Internode cross-sectional area was calculated using the area formula for an ellipse. These four internodes were immediately placed in 50% ethanol/water (v/v) for preservation until microscopic analysis could be conducted. The remaining internodes from each plot were frozen and lyophilized. The dried internode samples were ground to pass a 6-mm screen in a Wiley mill (Arthur H. Thomas Co., Philadelphia, PA) and then ground to pass a 1-mm screen in a cyclone mill.

Chemical Analysis

Dried and ground internode samples were analyzed for cell wall polysaccharide sugar residues and lignin by the Uppsala Dietary Fiber method (Theander et al., 1995). After preparation of a starch-free, alcohol insoluble residue the samples were dissolved in 12 M sulfuric acid at room temperature for 3 h, followed by dilution with water to 0.3 M sulfuric acid and heating in an autoclave at 121°C for 1 h to hydrolyze the cell wall polysaccharides. The insoluble Klason lignin residue was recovered by filtration, and neutral sugar residues (glucose, xylose, arabinose, mannose, galactose, rhamnose, and fucose) in the filtrate were quantified by gas chromatography as alditol acetate derivatives (Theander et al., 1995). Inositol was used as an internal standard to correct for volume variation. Neutral sugar data were converted to an anhydro-sugar basis. Total uronic acids were measured by colorimetry in aliquots of the 0.3 M sulfuric acid solution sampled before heating, using glucuronic acid as the reference standard (Ahmed and Labavitch, 1977). The Klason lignin residue was corrected for ash content by combustion in a muffle furnace for 6 h at 450°C.

Total (ester- and ether-linked) ferulates in the cell wall were extracted with 4 M NaOH for 3 h at 160°C from starch-free, alcohol insoluble residues (Iiyama et al., 1990). Ester-linked ferulates and p-coumarates were extracted from similar starch-free, alcohol insoluble residues with 2 M NaOH at 39°C for 24 h (Jung and Shalita-Jones, 1990). Ferulic and p-coumaric acid residues in the alkaline extracts were quantified by high-pressure liquid chromatography (Jung and Shalita-Jones, 1990). Ether-linked ferulate was calculated as the difference between total and ester-linked ferulic acid concentrations of each sample (Iiyama et al., 1990).

The composition of maize lignin was determined by pyrolysis-GC–MS analysis as described by Ralph and Hatfield (1991). The syringyl-to-guaiacyl monolignol ratio of lignin was calculated using data normalized for the guaiacol yield from each sample (Jung and Buxton, 1994).

Maize internode cell wall concentration was calculated as the sum of glucose, xylose, arabinose, mannose, galactose, rhamnose, fucose, uronic acids, Klason lignin, total ferulates, and ester-linked p-coumarate. All data were corrected to an organic matter (OM) basis by drying ground internodes samples overnight at 100°C and subsequent ashing at 450°C for 6 h.

Microscopic Analysis

The 50% ethanol-preserved internodes were used to examine patterns of tissue development. Based on differences observed for internode dimensions and chemical data among the hybrids and among the development stages, internodes from Sampling Dates 2, 4, 6, 8, and 10 were prepared for microscopic evaluation. Cross-sections 100 μm in thickness were made with a sliding-type microtome from the middle of the internodes. Several sections from each internode were stored in 50% ethanol for subsequent analysis.

Randomly chosen sections from each selected internode were mounted on slides with 50% glycerol and examined by light microscopy for cell wall development of individual maize stem tissues. A Spot digital camera (Diagnostic Instruments, Inc., Sterling Heights, MI) was used to collect images. Additional sections were stained with acid phloroglucinol before light microscopy to visualize the presence or absence of lignin in maize tissues (Jensen, 1962). The number of vascular bundles in rind and pith sections from Sampling Date 10 internodes was counted for each cross-section. Digital images were processed using Adobe Photoshop (Adobe Systems Inc., San Jose, CA) to improve contrast and annotate figures.

Statistical Analysis

Cell wall chemical composition analyses were done in duplicate. Mean physical measurements and chemical compo-

Table 1. Dates when the fourth elongated internode above ground level was sampled from three maize hybrids in 1998 and 1999, number of internodes collected from each field plot, and mean day of the year for each sampling. Cumulative growing degree days (10°C base) since planting are shown in parenthesis for each sampling date.

Sample	1998	1999	Number of internodes	Mean day of the year
One	24 June (688)	28 June (740)	44	177
Two	26 June (738)	30 June (768)	44	179
Three	28 June (785)	2 July (805)	34	181
Four	2 July (875)	6 July (920)	24	185
Five	6 July (959)	10 July (1006)	10	189
Six	13 July (1139)	16 July (1165)	10	196
Seven	20 July (1315)	23 July (1333)	8	203
Eight	3 August (1605)	6 August (1682)	8	217
Nine	31 August (2247)	3 September (2290)	8	245
Ten	28 September (2773)	1 October (2629)	8	273

sition data for internode samples were analyzed by mixed models analysis, using a randomized complete block design combined over years with sampling dates as repeated measures. The repeated measures were modeled using unstructured, compound symmetric, and heterogeneous compound symmetric covariance structures with the best structure chosen on the basis of Akaike's Information Criterion (SAS Institute Inc., Cary, NC). Grain and stover yields and vascular bundle numbers for rind, pith, and rind plus pith were analyzed by mixed models analysis, excluding the repeated measures factor. Hybrid and sampling date were treated as fixed effects, while year and block were treated as random effects. Means of fixed effects were compared using Fisher's least-significant difference (LSD). Mean squares used in the LSD calculations were synthesized as linear combinations of variance components for all random effects that contributed to a particular fixed effect (Littel et al., 1996). All effects presented in the Results section were significant at the $P < 0.05$ probability level.

RESULTS

Morphological Development

Mean daily air temperatures in 1998 and 1999 were very similar to the 30-yr average, with 1998 being warmer in May and September than was 1999 (Table 2). Cumulative growing degree days (10°C base) were similar between the two study years at all sampling dates, although 1999 was consistently higher for all sampling dates other than the last (Table 1). Both years had higher rainfall totals during the growing season than the 30-yr average. Precipitation was especially high in May and August of 1998, whereas 1999 had major rainfall events in May and July. Grain (252, 190, and 247 ± 42 g plant^{-1}) and stover (334, 336, and 282 ± 100 g plant^{-1}) yields did not differ among hybrids 632, 679, and 2677, respectively.

All three maize hybrids followed similar patterns of internode growth over both years of the study. Elongation of the internode ended between Sampling Dates 5 and 6 for all hybrids (Fig. 1a). While hybrids 679 and 2677 were generally similar in length of the internode throughout development, hybrid 632 reached and maintained a greater length for this specific internode than the other two hybrids from Sampling Date 3 onward. Growth in cross-sectional area of the internode was complete when elongation ended (Fig. 1b). Maize hybrid 2677 had a larger cross-sectional area than the other two hybrids, which were similar to one another, from Sampling Date 6 onward. No increases in internode length or cross-sectional area were observed after Sampling
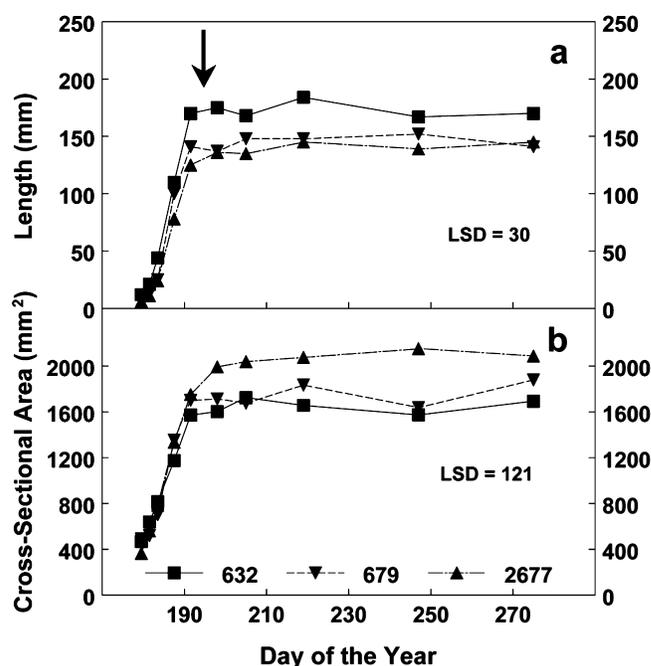

Fig. 1. Length (a) and cross-sectional area (b) of the fourth elongated internode above ground level for three maize hybrids (632, 679, and 2677), sampled on 10 dates during development, averaged across years. The arrow located between Sampling Dates 5 and 6 represents the approximate time when elongation of the internodes ceased. LSD, least significant difference ($P < 0.05$).

Date 6. Further development of the internodes was limited to secondary cell wall development of tissues over subsequent sampling dates.

Figure 2 shows an example of a typical stem cross-section, from a fully developed internode collected on Sampling Date 10, which was examined by light microscopy. The rind region contained numerous, closely-spaced vascular bundles embedded in small-diameter parenchyma tissue. In contrast, in the pith region vascular bundles were less numerous and parenchyma cells were larger. At this stage of full development, rind-region parenchyma had thicker walls, and more sclerenchyma cells surrounded the vascular bundles than observed for these tissues in the pith region (Fig. 2). In the area encompassed by double microscopic fields of view (~44 mm^2) there were no differences among hybrids 632, 679, and 2677 for total number of vascular bundles (27.5, 24.5, and 24.4 ± 1.7 bundles, respectively). Number

Table 2. Mean monthly air temperature and precipitation totals during the 1998 and 1999 growing seasons and the 30-yr average at the University of Minnesota St. Paul Campus.

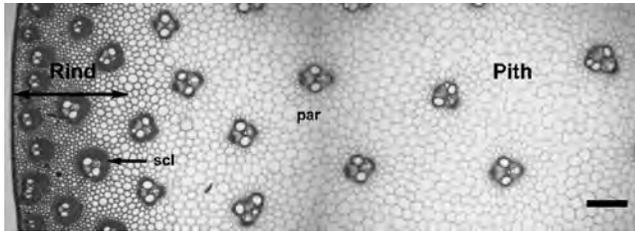|	Month						
	May	June	July	Aug.	Sept.	Mean	Total
	°C						
Mean air temperature							
30-yr average	14.7	20.1	23.1	21.4	15.8	19.0	
1998	19.2	18.7	22.8	22.4	20.2	20.7	
1999	16.8	20.2	24.9	21.5	17.0	20.1	
	mm						
Precipitation							
30-yr average	86	103	90	92	69		440
1998	105	180	53	153	56		547
1999	184	117	162	94	67		624

Fig. 2. A partial overview of a cross-section from the fourth elongated internode above ground level of maize hybrid 632 sampled at full maturity (Sampling Date 10). The image was made by combining two adjacent microscopic fields of view. The double-ended arrow marks the approximate width of the rind region, as determined by visual appraisal, based on the typical sclerenchyma thickening around vascular bundles and thickening of parenchyma cell walls in the rind. Bar = 500 μm, par = parenchyma, scl = sclerenchyma.

of rind- and pith-region vascular bundles also did not differ among the hybrids (data not shown).

The patterns of tissue development for the internode are illustrated in Fig. 3. At the earliest stages of development only protoxylem vessel cells had thick cell walls and this was the only tissue that stained positive for the presence of lignin. By Sampling Date 4 protoxylem vessels were still the only lignified tissue, but sclerenchyma cells surrounding some rind-region vascular bundles had begun to thicken. Growth in cell diameter, particularly for pith parenchyma, was evident by this sampling date. With the end of internode elongation by Sampling Date 6, the metaxylem had become lignified and sclerenchyma associated with vascular bundles had thickened and lignified. The phloem tissue in vascular bundles was not lignified and did not lignify as development continued. Parenchyma in the rind region had developed a thick and lignified secondary wall as post-elongation development proceeded to Sampling Date 8. A small number of lignified sclerenchyma cell clumps not directly associated with vascular bundles developed in the rind region and sclerenchyma also developed immediately under the epidermis. The parenchyma in the pith developed marginally thickened walls by Sampling Date 8 and stained positive for lignin; however, the first two or three cell layers immediately adjacent to pith-region vascular bundles consisted of small-diameter parenchyma cells that did not become lignified at any point during internode development.

Even though the maize hybrids did exhibit some consistent morphological differences in internode length and diameter, no obvious differences were noted among the hybrids in the patterns of tissue development based on the microscopic observations. Also, this morphological variation among hybrids did not result in any consistent differences in cell wall concentration and composition during the course of internode development (see following section).

Cell Wall Composition

The analysis of variance for cell wall traits indicated that hybrids did not differ, except for *p*-coumarate esters, but sampling date was significant for all cell wall traits (Table 3). The hybrid × sampling date interaction was
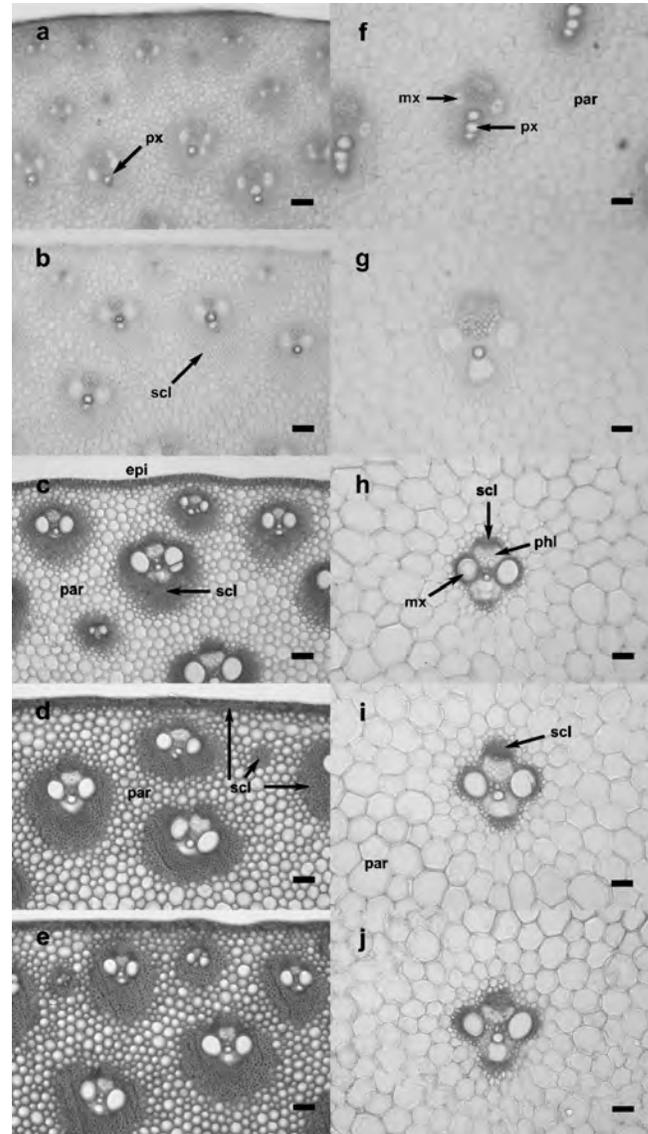

Fig. 3. Micrographs of maize stem cross-sections from the fourth elongated internode above ground level showing anatomical development at Sampling Dates 2, 4, 6, 8, and 10 of rind (a through e, respectively) and pith (f through j, respectively) tissues during internode development of hybrid 679. All micrographs are for internodes collected from the same field replicate block in 1998. Sections were stained for the presence of lignin using phloroglucinol, which is evident as darker cell walls in these gray-scale images. Bar = 100 μm, epi = epidermis, mx = metaxylem, par = parenchyma, phl = phloem, px = protoxylem, scl = sclerenchyma.

significant for most traits, and was largely due to numerous changes in ranking among the hybrids, with no stable or consistent differences among hybrids in cell wall concentration or composition across sampling dates (data not shown). Because sampling date accounted for the largest effect on cell wall development, and quantifying cell wall changes during internode development were the objective of this study, the following data presentation will focus only on differences among sampling dates.

Cell wall concentration of the fourth elongated internode above ground level was low at Sampling Date 1 (307 ± 6 g kg^{-1} OM) and did not change significantly

Table 3. Mixed models analysis results for fixed effects on length, area, and cell wall concentration and composition of the fourth elongated internode above ground level from three maize hybrids grown at St. Paul, MN in 1998 and 1999, sampled at 10 developmental stages.

Trait†	Fixed effect		
	Hybrid	Sampling date	Hybrid × date
Degrees of freedom	2	9	18
Length	NS‡	***	*
Area	NS	***	**
Cell wall	NS	***	*
Klason lignin	NS	**	*
Glucose	NS	***	NS
Xylose	NS	***	NS
Arabinose	NS	***	*
Galactose	NS	***	***
Mannose	NS	***	**
Rhamnose	NS	***	**
Uronic acids	NS	***	NS
Ferulate esters	NS	***	*
Ferulate ethers	NS	***	NS
p-Coumarate esters	*	***	***
Ara:Xyl	NS	***	NS
FA:Ara	NS	***	*
S:G	NS	***	*

* Probability level of 0.05.
** Probability level of 0.01.
*** Probability level of 0.001.
† Ara:Xyl, molar ratio of arabinose-to-xylose; FA:Ara, molar ratio of total ferulates-to-arabinose; S:G, syringyl-to-guaiacyl monolignol ratio.
‡ NS, nonsignificant ($P > 0.05$).

among Sampling Dates 1 through 3, but was followed by a rapid increase in concentration over Sampling Dates 4 through 6 (Fig. 4a). Across hybrids, maximum cell wall concentration occurred at Sampling Date 7 (733 ± 9 g kg^{-1} OM) followed by a decline until Sampling Date

9. In contrast, Klason lignin concentration declined from Sampling Dates 1 (109 ± 10 g kg^{-1} cell wall) to 4 (56 ± 13 g kg^{-1} cell wall), which was followed by an increase until Sampling Date 8 (195 ± 10 g kg^{-1} cell wall) in lignin concentration (Fig. 4a). At the most immature stage of development (Sampling Date 1), maize stem cell wall polysaccharides contained 349 ± 7 g glucose, 180 ± 3 g xylose, 100 ± 1 g arabinose, and 145 ± 2 g uronic acids kg^{-1} cell wall material. Cell wall glucose concentration of maize stem tissues increased with each successive sampling date until a maximum was reached at Sampling Date 4 (Fig. 4b). After the end of internode elongation by Sampling Date 6, glucose concentration of walls decreased with ensuing sampling dates until Sampling Date 8 when concentration of cell wall glucose stabilized. Xylose concentration in maize cell walls followed the same developmental pattern as glucose. In contrast to glucose and xylose, the remaining polysaccharide sugars (arabinose, galactose, mannose, rhamnose, and uronic acids) all declined from Sampling Date 1 to a minimum by Sampling Date 6. Fucose was the least abundant cell wall polysaccharide sugar, and was only detected in maize from Sampling Dates 1 and 2 (data not shown).

As ester- and ether-linked ferulates accumulated in cell walls, they followed similar patterns in cell wall concentration, but different timing (Fig. 5a). At Sampling Date 1, ferulate esters averaged 1.20 ± 0.04 g kg^{-1} cell wall and increased rapidly over successive sampling dates. A plateau in cell wall ferulate ester concentration was reached beginning at Sampling Date 4, although
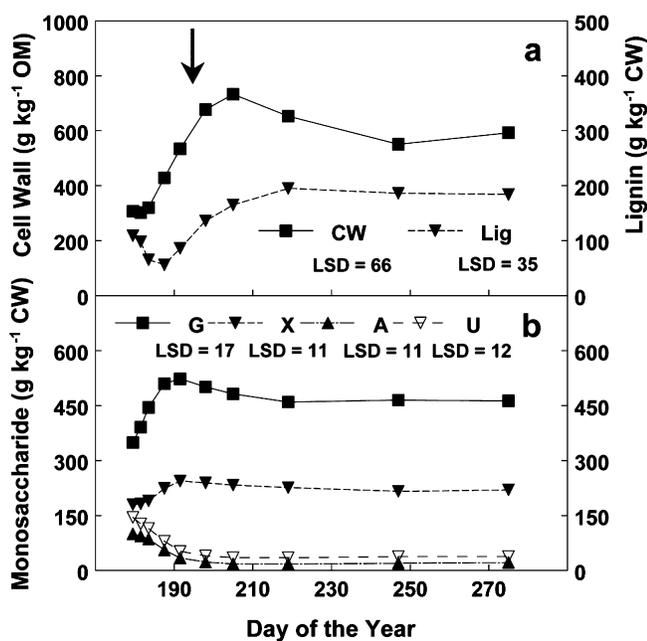

Fig. 4. Cell wall and Klason lignin concentrations (a) and cell wall concentrations of glucose (G), xylose (X), arabinose (A), and uronic acid (U) residues from cell wall polysaccharides (b) of the fourth elongated internode above ground level. Data were averaged across three maize hybrids and 2 yr, sampled on 10 dates during development. The arrow located between Sampling Dates 5 and 6 represents the approximate time when elongation of the internodes ceased. LSD, least significant difference ($P < 0.05$).
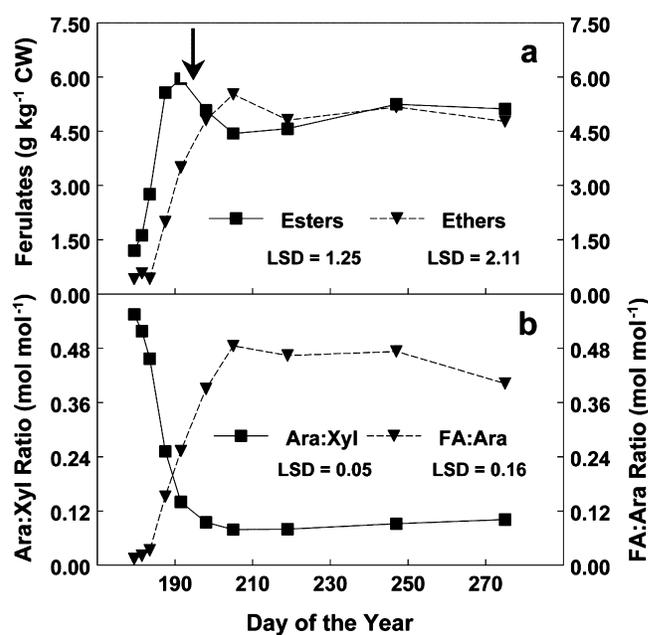

Fig. 5. Concentrations of ester- and ether-linked ferulates (a) and molar ratios of arabinose-to-xylose (Ara:Xyl) and total ferulates-to-arabinose (FA:Ara) (b) in the cell wall of the fourth elongated internode above ground level. Data were averaged across three maize hybrids and 2 yr, sampled on 10 dates during development. The arrow located between Sampling Dates 5 and 6 represents the approximate time when elongation of the internodes ceased. LSD, least significant difference ($P < 0.05$).

internodes from Sampling Dates 7 and 8 were lower than the maximum concentration observed at Sampling Date 5 (5.96 ± 0.10 g kg^{-1} cell wall). Etherified ferulates were present at very low concentration for Sampling Date 1 (0.41 ± 0.07 g kg^{-1} cell wall) and did not begin to increase in concentration until after Sampling Date 3. Ferulate ether concentration reached a statistical plateau from Sampling Date 5 onward, with a maximum numerical concentration of 5.52 ± 0.18 g kg^{-1} cell wall at Sampling Date 7.

The molar ratio of arabinose-to-xylose residues in maize cell wall polysaccharides was greater than 0.50 ± 0.01 at Sampling Date 1 (Fig. 5b). This ratio of sugar units declined progressively to 0.08 ± 0.01 at Sampling Date 7. The molar ratio for total ferulates-to-arabinose showed the opposite pattern (Fig. 5b). The ferulates-to-arabinose ratio began at 0.01 ± 0.001 at Sampling Date 1 and started to increase at Sampling Date 4, reaching a plateau by Sampling Date 7, with a maximum value of 0.48 ± 0.01 at Sampling Date 7. This ratio declined slightly at Sampling Date 10. The syringyl-to-guaiacyl monolignol ratio was extremely low for maize internodes from Sampling Dates 1, 2, and 3, but then increased sharply until Sampling Date 7, followed by a more gradual increase through Sampling Date 9 (Fig. 6). The concentration of p-coumarate esters in the cell wall followed a nearly identical pattern of increase to that seen for the syringyl-to-guaiacyl ratio.

DISCUSSION

Lignification of plant cell walls reduces degradability by rumen microorganisms (Jung and Deetz, 1993; Wilson, 1993); therefore, understanding which tissues lignify and when lignification occurs is critical. During internode elongation, microscopic observations in the current study clearly showed that only nonlignified cell
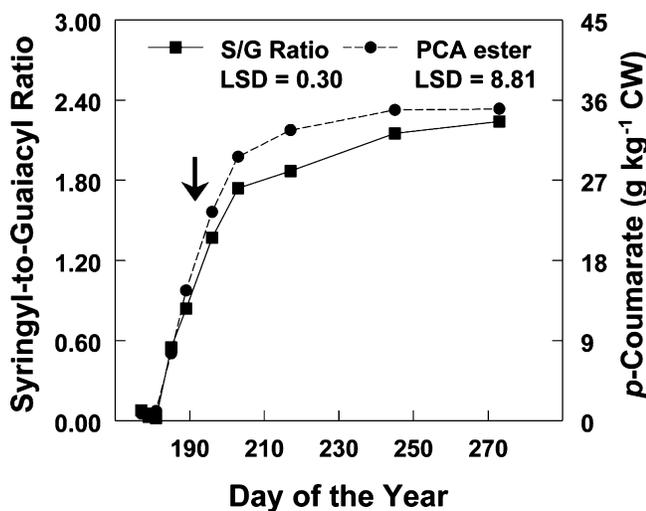

Fig. 6. Mean ratio of syringyl-to-guaiacyl monolignol units (S/G) in lignin and concentration of p-coumarate (PCA) esters in the cell wall of the fourth elongated internode above ground level. Data were averaged across three maize hybrids and 2 yr, sampled on 10 dates during development. The arrow located between Sampling Dates 5 and 6 represents the approximate time when elongation of the internodes ceased. LSD, least significant difference ($P < 0.05$).

wall material was present on Sampling Date 1, other than protoxylem vessels which were already lignified at Sampling Date 1. None of the other stem tissues stained positive for lignin with phloroglucinol during the internode elongation phase. In very young elongating internodes of tall fescue (*Festuca arundinacea* Schreb.), protoxylem vessels were also the only tissue to stain for the presence of lignin, using the Maule and Safranin-*O* stains (Chen et al., 2002). The localization of lignin to only protoxylem vessels in elongating internodes is apparently a general feature of stem development in forages as it has also been observed in alfalfa (Jung and Engels, 2002).

The current composition data showed limited lignin concentrations in the youngest maize internode and even indicated a decline in lignin as a proportion of the cell wall during early elongation, although lignin concentration did begin increasing before the cessation of elongation. Morrison et al. (1994) observed that tissues at the top of an elongating maize internode had begun to lignify before elongation was complete. Because the chemical data in the current study were derived from whole internodes, the shift toward secondary wall development and lignification before elongation was complete probably reflects the greater development of tissues at the top of the internode rather than tissues lower on the internode, consistent with the basipetal pattern of grass internode growth (Kaufman et al., 1965).

The decline in lignin concentration between Sampling Dates 1 and 4 suggests that protoxylem vessels in the youngest internode accounted for more of the internode's total cell wall material relative to the other, nonlignified tissues than was the case at subsequent sampling dates. Over Sampling Dates 5 through 7, nonlignified primary wall material was added by growing cells in nonlignified tissues, thereby diluting the overall lignin concentration of internode cell wall material. Large and rapid increases in cell wall concentration and lignification immediately after cessation of internode elongation were associated with development of thick, lignified secondary walls in sclerenchyma, rind-region parenchyma, and epidermal tissues. While lignin concentration of the cell wall continued to increase until Sampling Date 8, cell wall concentration declined from Sampling Date 7 through 9. However, it was evident that rind-region parenchyma developed thickened and lignified walls during this interval, along with additional secondary wall thickening of sclerenchyma. Because total amount of cell wall material in the internode continued increasing through Sampling Date 9 (Jung, 2003), the decrease in cell wall concentration later in post-elongation development was most likely due to accumulation of sucrose and starch in the stem, thereby diluting cell wall concentration (Dwyer et al., 1995).

Determination of actual mass and cell wall concentration of individual stem tissues is difficult. In sorghum [*Sorghum bicolor* (L.) Moench], physical dissection of the fifth internode from the top of the plant was done at anthesis and grain maturity (Wilson et al., 1993). Based on cross-sectional area, the pith parenchyma accounted for 80% of the stem area at both maturity stages. How-

ever, as a percent of total cell wall (estimated as neutral detergent fiber) the pith parenchyma only contributed about 21% of the internode's cell wall material. In contrast, the rind-region vascular bundle zone (vascular bundles, sclerenchyma, and parenchyma) contributed 54 and 52% of the cell wall material in this sorghum internode at anthesis and grain maturity, respectively, compared to only 12 to 14% of the cross-sectional area (Wilson et al., 1993). These observations support the conclusion from the current study that extensive secondary wall development of sclerenchyma and parenchyma in the rind region contributed heavily to cell wall accumulation of the maize internode after the cessation of elongation. However, unlike in alfalfa internodes where many tissues remain non-lignified during stem development (Engels and Jung, 1998; Jung and Engels, 2002), all internode tissues in maize, except phloem, became lignified.

Data on cell wall composition of individual forage tissues is very limited. Lignin concentration of sorghum pith parenchyma cell walls was slightly lower than pith-region vascular bundles (Hatfield et al., 1999). Also in sorghum, rind-region vascular tissue cell walls were similar to pith tissues in lignin concentration at anthesis, but increased by grain maturity. The epidermis and sub-epidermal sclerenchyma had the most heavily lignified walls in sorghum tissues (Hatfield et al., 1999). Orchardgrass (*Dactylis glomerata* L.) and switchgrass (*Panicum virgatum* L.) leaf blade, sheath, and stem were fractionated into parenchyma and sclerenchyma tissue by maceration and sieving (Grabber and Jung, 1991). Lignin concentration of orchardgrass cell walls was greater in sclerenchyma tissue than parenchyma for all plant parts; however, switchgrass leaf and stem parenchyma cell walls contained more lignin than did sclerenchyma (Grabber et al., 1991). From this literature and the current observations it is not possible to speculate as to which rind-region tissues account for the majority of the lignin in maize internodes.

The data showing that ferulate ether concentration began to rise later during elongation than ferulate esters supports the concept that ferulate esters of arabinoxylan are deposited in the primary wall of grasses and ether cross-links to lignin form later (Ralph et al., 1998). In wheat (*Triticum aestivum* L.) stems, the proportion of etherified versus esterified ferulates increased from the youngest internode segment (bottom) to the next higher segment of a newly elongated internode, but remained constant in subsequent older internode segments (Iiyama et al., 1990). This pattern mirrored the results in the current study and followed the same trend as observed using internode position to provide a developmental profile for cell wall ferulates (Morrison et al., 1998). Jung (2003) showed that deposition of ferulate esters is not limited to primary walls, contrary to an earlier hypothesis (Jung and Deetz, 1993), and approximately 60% of ferulates are present in the secondary wall material of maize.

Ferulates are present in grass cell walls as esters of arabinose units on xylans, and many of the ferulate molecules become involved in cross-links between arabi-noxylans by formation of diferulate bridges and/or as nucleation sites for the lignin deposition (Ralph et al., 1998). Both diferulate cross-linking of arabinoxylans and cross-linking of lignin to arabinoxylan have been shown to reduce maize cell wall degradability (Grabber et al., 1998a, 1998b). As xylans became less substituted with arabinose units during development of the maize internode, the degree of substitution of the arabinose with ferulates increased dramatically from 1 to over 45%. The same general trend was observed for segmented maize internodes where ester-linked ferulates on arabinose units increased from about 9 to more than 35% substitution (Scobbie et al., 1993). This high level of ferulate substitution of arabinose units in secondary walls of older tissues suggests many opportunities exist for formation of lignin/arabinoxylan cross-links; however, diferulate linkages between arabinoxylans molecules would be less likely in secondary walls if the arabinose substitutions were relatively evenly spaced on the xylans because of the low arabinose-to-xylose ratio observed for the old internodes. It appears that a shift from xylans highly substituted with arabinose to low arabinose substitution rates of xylans is a general phenomenon of cell wall development in grass tissues (Morrison, 1974, 1980; Scobbie et al., 1993). Unfortunately diferulates could not be quantified in the current study because of the non-availability of the many diferulate compounds needed as standards.

It is well established that grasses deposit syringyl-rich lignin during secondary wall development (Terashima et al., 1993). The current study reinforces this observation and also supports the conclusion of Ralph et al. (1994) that most *p*-coumarate esters in maize are on syringyl monolignol units. Concentration of *p*-coumarates in the cell wall increased dramatically during maize secondary wall development and followed the same trajectory as the syringyl-to-guaiacyl monolignol ratio. While both lignin composition and *p*-coumarate esters of lignin can be negatively correlated with cell wall degradability of grasses (Jung and Deetz, 1993), it is not clear that these cell wall characteristics directly impact degradability or if these relationships arise out of co-incidental developmental changes to plant cell walls (Chesson, 1993; Jung et al., 1999).

CONCLUSION

Three conventional, non-related maize hybrids all exhibited a similar pattern for stem tissue and cell wall development even though significant differences in internode length and cross-sectional area were observed among the hybrids. During internode elongation, protoxylem was the only stem tissue that was lignified. Secondary wall thickening and lignification began after internode elongation was complete. At physiological maturity, phloem was the only tissue in maize stems that was uniformly not lignified, although some pith-region parenchyma immediately adjacent to vascular bundles was also non-lignified. This pattern of cell wall lignification was in marked contrast to alfalfa where most types of stem tissues did not lignify during development.

The marked increase in cell wall concentration that occurred during internode development was largely associated with secondary wall development of rind-region sclerenchyma and parenchyma tissues. Genetic efforts to reduce cell wall concentration and/or lignification should focus on these rind tissues.

REFERENCES

Ahmed, A.E.R., and J.M. Labavitch. 1977. A simplified method for accurate determination of cell wall uronide content. J. Food Biochem. 1:361–365.

Akin, D.E. 1989. Histological and physical factors affecting digestibility of forages. Agron. J. 81:17–25.

Aman, P., and E. Lindgren. 1983. Chemical composition and in vitro degradability of individual chemical constituents of six Swedish grasses harvested at different stages of maturity. Swed. J. Agric. Res. 13:221–227.

Buxton, D.R. 1989. In vitro digestion kinetics of temperate perennial forage legume and grass stems. Crop Sci. 29:213–219.

Chen, L., C. Auh, F. Chen, X. Cheng, H. Aljoe, R.A. Dixon, and Z. Wang. 2002. Lignin deposition and associated changes in anatomy, enzyme activity, gene expression, and ruminal degradability in stems of tall fescue at different developmental stages. J. Agric. Food Chem. 50:5558–5565.

Chesson, A. 1993. Mechanistic models of forage cell wall degradation. p. 347–376. In H.G. Jung et al. (ed.) Forage cell wall structure and digestibility. ASA, CSSA, and SSSA, Madison, WI.

Dwyer, L.M., C.J. Andrews, D.W. Stewart, B.L. Ma, and J.-A. Dugas. 1995. Carbohydrate levels in field-grown leafy and normal genotypes. Crop Sci. 35:1020–1027.

Engels, F.M., and H.G. Jung. 1998. Alfalfa stem tissues: Cell-wall development and lignification. Ann. Bot. (Lond.) 82:561–568.

Grabber, J.H., and G.A. Jung. 1991. Isolation of parenchyma and sclerenchyma cell types from the plant parts of grasses. Crop Sci. 31:838–842.

Grabber, J.H., G.A. Jung, and R.R. Hill, Jr. 1991. Chemical composition of parenchyma and sclerenchyma cell walls isolated from orchardgrass and switchgrass. Crop Sci. 31:1058–1065.

Grabber, J.H., R.D. Hatfield, and J. Ralph. 1998a. Diferulate cross-links impede the enzymatic degradation of non-lignified maize walls. J. Sci. Food Agric. 77:193–200.

Grabber, J.H., R.D. Hatfield, and J. Ralph. 1998b. Ferulate cross-links limit the enzymatic degradation of synthetically lignified primary walls of maize. J. Agric. Food Chem. 46:2609–2614.

Hatfield, R.D., J.R. Wilson, and D.R. Mertens. 1999. Composition of cell walls isolated from cell types of grain sorghum stems. J. Sci. Food Agric. 79:891–899.

Iiyama, K., T.B.T. Lam, and B.A. Stone. 1990. Phenolic acid bridges between polysaccharides and lignin in wheat internodes. Phytochemistry 29:733–737.

Jensen, W.A. 1962. Botanical histochemistry. Freeman and Co., San Francisco.

Jung, H.G. 2003. Maize stem tissues: Ferulate deposition in developing internode cell walls. Phytochemistry 63:543–549.

Jung, H.G., and D.R. Buxton. 1994. Forage quality variation among maize inbreds: Relationships of cell-wall composition and in vitro degradability for stem internodes. J. Sci. Food Agric. 66:313–322.

Jung, H.G., and M.D. Casler. 2006. Maize stem tissues: Impact of maturation on cell wall degradability. Crop Sci. 46:1801–1809.

Jung, H.G., and D.A. Deetz. 1993. Cell wall lignification and degradability. p. 315–346. In H.G. Jung et al. (ed.) Forage cell wall structure and digestibility. ASA, CSSA, and SSSA, Madison, WI.

Jung, H.G., and F.M. Engels. 2001. Alfalfa stem tissues: Rate and extent of cell-wall thinning during ruminal degradation. Neth. J. Agric. Sci. 49:3–13.

Jung, H.G., and F.M. Engels. 2002. Alfalfa stem tissues: Cell-wall deposition, composition, and degradability. Crop Sci. 42:524–534.

Jung, H.G., W. Ni, C.C.S. Chapple, and K. Meyer. 1999. Impact of lignin composition on cell-wall degradability in an Arabidopsis mutant. J. Sci. Food Agric. 79:922–928.

Jung, H.G., and S.C. Shalita-Jones. 1990. Variation in the extractability of esterified p-coumaric and ferulic acids from forage cell walls. J. Agric. Food Chem. 38:397–402.

Jung, H.G., R.R. Smith, and C.S. Endres. 1994. Cell-wall composition and degradability of stem tissue from lucerne divergently selected for lignin and in vitro dry matter disappearance. Grass Forage Sci. 49:1–10.

Kaufman, P.B., S.J. Cassell, and P.A. Adams. 1965. On the nature of intercalary growth and cellular differentiation in internodes of Avena sativa. Bot. Gaz. (Chicago) 126:1–13.

Littel, R.C., G.A. Milliken, W.W. Stroup, and R.D. Wolfinger. 1996. SAS systems for mixed models. SAS Inst., Cary, NC.

Morrison, I.M. 1974. Changes in the hemicellulose polysaccharides of rye-grass with increasing maturity. Carbohydr. Res. 36:45–51.

Morrison, I.M. 1980. Changes in the lignin and hemicellulose concentrations of ten varieties of temperate grasses with increasing maturity. Grass Forage Sci. 35:287–293.

Morrison, T.A., H.G. Jung, D.R. Buxton, and R.D. Hatfield. 1998. Cell-wall composition of maize internodes of varying maturity. Crop Sci. 38:455–460.

Morrison, T.A., J.R. Kessler, and D.R. Buxton. 1994. Maize internode elongation patterns. Crop Sci. 34:1055–1060.

Ralph, J., and R.D. Hatfield. 1991. Pyrolysis-GC-MS characterization of forage materials. J. Agric. Food Chem. 39:1426–1437.

Ralph, J., R.D. Hatfield, J.H. Grabber, H.G. Jung, S. Quideau, and R.F. Helm. 1998. Cell wall cross-linking in grasses by ferulates and diferulates. p. 209–236. In N.G. Lewis and S. Sarkanen (ed.) Lignin and lignan biosynthesis. ACS, Washington, DC.

Ralph, J., R.D. Hatfield, S. Quideau, R.F. Helm, J.H. Grabber, and H.G. Jung. 1994. Pathway of p-coumaric acid incorporation into maize lignin as revealed by NMR. J. Am. Chem. Soc. 116:9448–9456.

Ritchie, S.W., J.J. Hanway, and G.O. Benson. 1989. How a corn plant develops. Iowa State University, Ames.

Scobbie, L., W. Russell, G.J. Provan, and A. Chesson. 1993. The newly extended maize internode: A model for the study of secondary cell wall formation and consequences for digestibility. J. Sci. Food Agric. 61:217–225.

Terashima, N., K. Fukushima, L.-F. He, and K. Takabe. 1993. Comprehensive model of the lignified plant cell wall, p. 247–270, In H.G. Jung et al. (ed.) Forage cell wall structure and digestibility. ASA, CSSA, and SSSA, Madison, WI.

Theander, O., P. Aman, E. Westerlund, R. Andersson, and D. Pettersson. 1995. Total dietary fiber determined as neutral sugar residues, uronic acid residues, and Klason lignin (The Uppsala Method): Collaborative study. J. AOAC Int. 78:1030–1044.

Wilson, J.R. 1993. Organization of forage plant tissues. p. 1–32. In H.G. Jung et al. (ed.) Forage cell wall structure and digestibility. ASA, CSSA, and SSSA, Madison, WI.

Wilson, J.R., D.R. Mertens, and R.D. Hatfield. 1993. Isolates of cell types from sorghum stems: Digestion, cell wall and anatomical characteristics. J. Sci. Food Agric. 63:407–417.